

# Identification of $\beta$ -strand mediated protein-protein interaction inhibitors using ligand-directed fragment ligation

Zsófia Hegedüs<sup>1</sup>, Fruzsina Hóbor<sup>2,3</sup>, Deborah K. Shoemark<sup>4,5</sup>, Sergio Celis<sup>1</sup>, Lu-Yun Lian<sup>6</sup>, Chi H. Trinh<sup>2,3</sup>, Richard B. Sessions<sup>4,5</sup>, Thomas A. Edwards<sup>2,3</sup>, Andrew J. Wilson<sup>1,2\*</sup>

<sup>1</sup>School of Chemistry, University of Leeds, Woodhouse Lane, Leeds LS2 9JT, UK, <sup>2</sup>Astbury Centre for Structural Molecular Biology, University of Leeds, Woodhouse Lane, Leeds LS2 9JT, UK, <sup>3</sup>School of Molecular and Cellular Biology, University of Leeds, Woodhouse Lane, Leeds LS2 9JT, UK, <sup>4</sup>School of Biochemistry, Biomedical Sciences Building, University of Bristol, Bristol, BS8 1TD, UK, <sup>5</sup>BrisSynBio, University of Bristol, Life Sciences Building, Tyndall Avenue, Bristol BS8 1TQ, UK, <sup>6</sup>Institute of Integrative Biology, University of Liverpool, Liverpool L69 3BX, UK,

**KEYWORDS:** protein-protein interactions, PDZ domain, hybrid structures, fragment-based drug discovery,  $\beta$ -sheets, acylhydrazone exchange

**ABSTRACT:**  $\beta$ -Strand mediated protein-protein interactions (PPIs) represent underexploited targets for chemical probe development despite representing a significant proportion of known and therapeutically relevant PPI targets.  $\beta$ -strand mimicry is challenging given that both amino acid side-chains and backbone hydrogen-bonds are typically required for molecular recognition, yet these are oriented along perpendicular vectors. This paper describes an alternative approach using GKAP/SHANK1 PDZ as a model and dynamic ligation screening to identify small-molecule replacements for tranches of peptide sequence. A peptide truncation of GKAP functionalized at the N- and C-termini with acylhydrazone groups was used as an anchor. Reversible acylhydrazone bond exchange with a library of aldehyde fragments in the presence of the protein as template and *in situ* screening using a fluorescence anisotropy (FA) assay identified peptide hybrid hits with comparable affinity to the GKAP peptide binding sequence. Identified hits were validated using FA, ITC, NMR and X-ray crystallography to confirm selective inhibition of the target PDZ-mediated PPI and mode of binding. These analyses together with molecular dynamics simulations demonstrated the ligands make transient interactions with an unoccupied basic patch through electrostatic interactions, establishing proof-of-concept that this unbiased approach to ligand discovery represents a powerful addition to the armory of tools that can be used to identify PPI modulators.

## INTRODUCTION

Protein-protein interactions (PPIs) play an essential role in the majority of biological processes and therefore represent arbiters of health and disease.<sup>1,2</sup> Chemical probes for PPIs offer tremendous opportunities to understand PPIs and therefore biological mechanisms whilst providing starting points for drug-discovery.<sup>3</sup> Conventional ligand discovery methods have delivered PPI modulators for a number of targets<sup>4-6</sup> leading to clinically approved drugs<sup>7</sup> such as Venetoclax (ABT-199). However, despite the enormous opportunity offered by PPIs, methods to identify modulators of PPIs remain underdeveloped. Peptide interacting motifs represent promising templates for design given they are likely to mediate a significant proportion of PPIs<sup>8</sup>; however, selecting the most appropriate scaffold to inhibit a specific PPI is highly dependent on the properties of the target interaction and varies in difficulty across PPI classes.<sup>9,10</sup> There has been considerable success in developing generic approaches to mimic the  $\alpha$ -helix and inhibit  $\alpha$ -helix mediated PPIs (e.g. using peptides, constrained peptides and peptidomimetics), but less so for other PPI topographies.<sup>11,12</sup> In particular,  $\beta$ -strand/ $\beta$ -sheet mediated PPIs exhibit a more complex topography and have proven more challenging; these interfaces are shallower and more elongated with backbone hydrogen bonding contributing significantly to the binding energy.<sup>13</sup> Scaffolds that mimic  $\beta$ -strands/ $\beta$ -sheets<sup>14-19</sup> have hitherto seen limited application<sup>20-22</sup> in PPI inhibitor discovery.<sup>23-28</sup>

In this work, we take a novel approach to  $\beta$ -strand mimicry whereby a truncated peptide-interacting motif is combined with a small-molecule fragment (Figure 1a), to generate a Class D (i.e. functional) mimetic.<sup>29</sup> As a screening approach, this offers the advantage of exploiting a peptide with intrinsic target affinity as an anchor to permit identification of weakly binding fragments. A related principle has been exploited in the REPLACE strategy whereby – aided by *in silico* methods – key residues of known peptide ligands were “mutated” for molecular fragments to identify inhibitors of conventional drug discovery targets e.g. kinases.<sup>30-34</sup> Subsequently, extension of this concept to  $\alpha$ -helix mediated PPIs has been achieved by screening peptide-small molecule hybrids *in silico*, then preparing promising candidates for experimental validation using click chemistry.<sup>35,36</sup> In this work, we instead use reversible hydrazone formation between peptide hydrazones and an aldehyde library together with dynamic ligation screening<sup>37,38</sup> to identify peptide-fragment hybrids. Such dynamic, template assisted methods shift thermodynamic equilibria in favor of the highest affinity ligands<sup>37-41</sup> and can target unoccupied binding sites<sup>42</sup> in an unbiased manner; they have proven successful for discovery of active site inhibitors,<sup>43-45</sup> but not been applied to PPI inhibitor discovery.

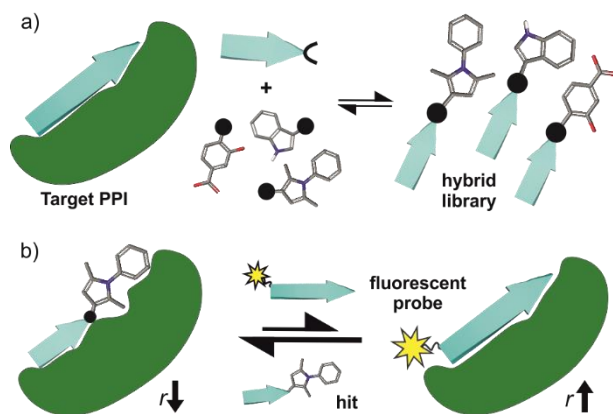


**Figure 1.** Design and screening strategy for identification of hybrid inhibitors. Schematic depicting the design strategy for identification of small molecule-peptide hybrids using a truncated anchor peptide derived from a known interaction partner of the protein target, and b) Schematic depicting fluorescence anisotropy ( $r$ ) competition assay-based screen for the identification of hit compounds that compete with a fluorescently labelled ligand at the target binding site.

As a model  $\beta$ -strand mediated PPI, we use the GKAP/SHANK-PDZ<sup>46</sup> which, plays a role in the organization of synaptic protein complexes and has been linked to several neuronal disorders.<sup>47</sup> There are > 250 PDZ domains with several therapeutically relevant proteins known to exhibit their function through a PDZ mediated interaction.<sup>48–50</sup> Ligand discovery for PDZ domains has proven challenging (e.g. fragment-based screening was unsuccessful for the PDZ domain of PSD-95<sup>51</sup>), with the majority of potent ligands based on protein<sup>52,53</sup>, peptide<sup>54,55</sup> or peptidomimetic scaffolds<sup>26,56–58</sup> and limited examples of small-molecules.<sup>59–62</sup> This rendered the GKAP/SHANK-PDZ interaction as a stringent test for our dynamic ligation screening approach. Using a three-residue sequence from the GKAP ligand, C- and N-terminal hydrazones were generated, then peptide-fragment hybrid assembly under neutral conditions performed in the presence of protein as a template and directly coupled to a fluorescence-based biophysical assay (Figure 1b). Characterization of the most promising hits using ITC, NMR, X-ray crystallography and molecular dynamics simulations established the hits as selective SHANK1 PDZ ligands (in comparison to PSD-95) with comparable potency to the GKAP PDZ-binding motif (PBM) (Ac-EAQTRL-COOH, hereafter simply referred to as GKAP) from which they were derived. Potency was achieved by binding to a cluster of basic residues proximal to the peptide binding site on the PDZ domain. These results thus establish dynamic ligation screening as a powerful tool to identify  $\beta$ -strand peptide-fragment mimetics as PPI inhibitors and broaden the scope of design strategies for PPI inhibitor discovery.

## RESULTS AND DISCUSSION

**Hybrid library design.** We chose acylhydrazone bond formation to covalently link fragments to peptide anchors (Figure 2a). In the presence of aminophenyl additives, the reaction can be performed close to neutral

pH, allowing the screening close to a physiologically relevant pH and temperature with the protein as a template for product formation.<sup>63,64</sup> Moreover, at neutral pH acylhydrazones are stable, facilitating subsequent hit validation.<sup>65,66</sup> Given the commercial availability of a large array of aldehydes, we thus designed the hybrids to be formed from peptide hydrazides.

Peptide anchors were designed based on the key features of the interaction between the wild type GKAP sequence and SHANK1 PDZ.<sup>46</sup> Class I PDZ domains bind to consensus sequences with a Thr/Ser in the -2 position from the C-terminus, a C-terminal hydrophobic residue and free carboxylate as the main determinants of affinity.<sup>67,68</sup> The plasticity of PDZ domains allows the accommodation of various hydrophobic side-chains at the C terminus of the peptide,<sup>69</sup> which we hypothesized to be an ideal target site for hydrophobic fragments; for SHANK1, Leu dominates for C-terminal carboxylates and Phe for non-C-terminal sequences.<sup>70</sup> This led to compounds **1** and **2** (Figure 2b, Scheme S1), directing the fragments toward the C-terminal hydrophobic pocket on SHANK1 PDZ. On the other hand, compounds **3** and **4** contained the TRL-COOH core sequence and the hydrazide functionality was attached to the N-terminus of the peptide through a 2 or 3 carbon atom linker (Figure 2c, Scheme S2), allowing exploration of the protein surface for secondary binding sites further away from the key residues. To ease purification, all peptide hydrazides were reacted with benzaldehyde, yielding the corresponding acylhydrazones (**1-**, **2-**, **3-**, **4-A001**)

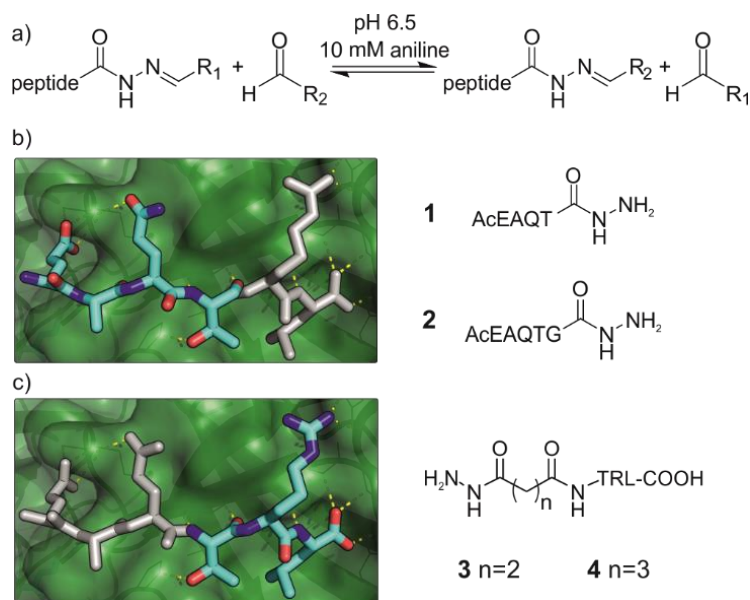


**Figure 2. Design principles for the anchor peptides based on the GKAP/SHANK1 PDZ interaction.** a) General reaction scheme for acylhydrazone exchange using peptide hydrazones and aldehydes in the presence of 10 mM aniline at pH 6.5. Anchor peptides generated from the GKAP sequence (cyan) based on its binding properties to SHANK1 PDZ (green, 1Q3P), truncated either from b) the C terminus or c) the N terminus. Residues outlined in white indicate the truncated amino acids and the fragment-targeting binding site.

A diversity-based selection was performed on commercially available aldehyde fragments obeying guidelines for fragment-based drug design,<sup>71</sup> resulting in a small library of 129 compounds (A001-A129, Table S1, Figure S1). Acylhydrazone formation was tested in the presence of 10 mM aniline<sup>63</sup> at pH 6.5 using a 5-fold excess of the competing aldehydes, which revealed fast and complete exchange of the benzaldehyde motif (Figure S2), reaching equilibrium within 24 hours. To allow us to perform the hybrid formation and screening in the presence of the target protein in a single step, it was necessary to first establish that SHANK1 PDZ was still able to bind to its natural ligand under the same conditions. For this FITC labelled GKAP was used and the fluorescence anisotropy measurements gave an initial  $K_D$  of  $\sim 1 \mu\text{M}$ , which did not significantly change over the course of 24 hours (Figure S3).

**Library screening.** Prior to screening, the intrinsic inhibitory potency of the peptide hydrazones **1-**, **2-**, **3-**, **4-A001** was determined (Figure S4). Then, hybrid formation and screening were performed by mixing each of these compounds at 10 or 50  $\mu\text{M}$  concentration with 5 equivalents of the aldehydes in a 384 well microtiter plate. After 24 hours of equilibration in the presence of SHANK1 PDZ protein, FITC-Ahx-TRL-OH was added as competitor. In all assays, the GKAP PBM sequence (Ac-EAQTRL-COOH), Ac-TRL-OH and a buffer control were used, which facilitated determination of threshold values for the hit compounds (Figure 3a, S5-6). Any hybrid that exceeded the activity of its parent compound was considered an improvement caused by the replacement of the fragment.

The two different truncation strategies had a profound effect on hit rates, reflecting the affinity of the parent compounds. The removal of the key C terminal residue of GKAP did not result in detectable binding affinity for the parent compounds **1-A001** and **2-A001** (Figure S4); our hypothesis was that a hybrid with a fragment effectively mimicking the truncated sequence could result in detectable affinity. Our library did not contain such fragments; hit rates were low, perhaps reflecting the challenge in attaining the correct orientation and composition of functionality needed to faithfully mimic the key interactions afforded by the natural truncated sequence. The solitary confirmed hit (Figure S7) appeared to interfere with the assay and was not considered further.

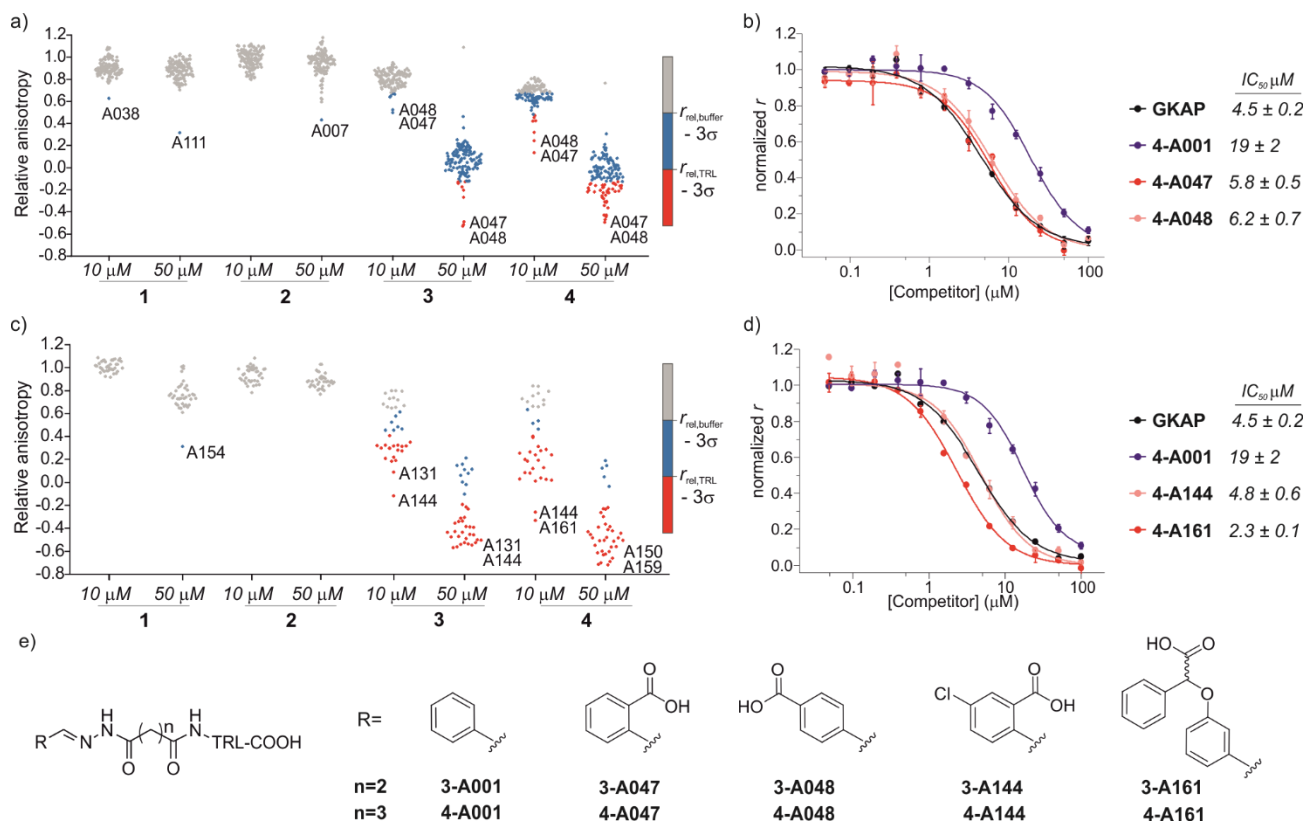


**Figure 3.** Results of the fluorescence anisotropy competition screening for compounds 1-4. a) Screening results for hydrazones formed from 1-4 using the diverse screening library (A001-A129). b) FA competition curves of the best hybrid hits. c) Screening results using the extended library including near neighbors (A130-165) for the initial hits. d) FA competition curves for hybrids from the extended screen. All screening and validation assays were performed in 50 mM  $\text{NH}_4\text{Ac}$  buffer, pH 6.5, 10 mM aniline using 1  $\mu\text{M}$  final protein concentration and 10 nM FITC-Ahx-TRL-COOH as tracer at room temperature. Compounds 1-, 2-, 3-, 4-A001 were incubated individually with 5 equivalents of fragments in the presence of SHANK1 PDZ for 24 hours. Anisotropy is expressed relative to the control experiment where no competitor is present. Hit thresholds were defined based on the relative anisotropy of the i) buffer control ( $r_{\text{buffer}}-3\sigma$ ) and ii) the TRL control ( $r_{\text{TRL}}-3\sigma$ ). Compounds below these thresholds are colored blue and red respectively. Labels indicate the two best aldehyde fragment hits from the individual screens. For individual values and FA validation for additional hits see Supporting information Figures S5-12. e) Structures of the synthesized hit compounds.

On the other hand, using compounds 3-A001 and 4-A001 with intrinsic potency (Figure S4) resulted in a higher hit rate (Figure 3a, Figure S5-6), with 51 hybrids exceeding the activity of Ac-TRL-COOH, which was the core motif in both hybrid sequences. The most promising hits were re-tested in order to validate the screening assay (Figure 3b and S8-9). The  $IC_{50}$  values measured for the best hits were in the range of 5-6  $\mu\text{M}$ , a 10-fold improvement compared to the parent Ac-TRL-COOH sequence, indicating that covalent attachment of the fragment contributes favorably to interaction with the protein. Interestingly, the most potent hybrids formed from 3 and 4 contained the same carboxylic acid functionalized aromatic aldehyde fragments (A047 and A048, Figure 3b), indicating that these types of fragments might play an important role in binding.

Based on this observation, we extended the aldehyde library to near neighbors of these fragments and selected an additional 36 carboxylic acid functionalized aromatic aldehydes (A130-165, Figure S1, Table S1) with which to carry out a further screen. In this extended screen, the hit rate increased significantly (Figure 3c,d and S10-12), confirming that an acidic binding motif is generic for favorable binding and confirming they could not have been identified without conjugation to the anchor peptides.

In the subsequent validation, the  $IC_{50}$  values of the best hits (formed from compound **4** and A144 or A161) reached or slightly exceeded the binding affinity of full length GKAP peptide, indicating that the fragment can restore the affinity of the truncated sequence to that of the wild-type peptide. Significantly, all but one of the aldehyde fragments showed no inhibitory capability on their own in the assay (Figure S13).

**Structure-activity relationships.** To establish structure-activity relationships, the most active hybrids were synthesized individually (Figure 3e, Scheme S2) and subjected to further characterization by isothermal titration calorimetry (ITC) (see Figure S14). The truncation of the GKAP sequence ( $K_D = 2 \pm 0.3 \mu\text{M}$ ) to its core TRL motif ( $K_D = 22 \pm 3 \mu\text{M}$ ) resulted in a decrease in affinity (Figure 4, Table 1). This was accompanied by the loss of binding enthalpy but also resulted in a more favorable entropy of binding (Table 1), presumably due to the loss of rotatable bonds on amino acid removal. Hydrazones formed from benzaldehyde and this core motif (compounds **3-A001** and **4-A001**) revealed slightly increased affinity than the TRL motif (Figure 4, Table 1), which might be the result of favorable interaction of the aromatic fragment or the hydrazone bond itself with the protein. Hybrid hits in which the fragments contained the additional carboxylic acid functional group resulted in increased binding affinity in every case (Figure 4, Table 1), which confirmed the importance of the acidic group and that these fragments actively contribute to SHANK1 binding. Interestingly, hybrids with the C3 linker (compound **4** hydrazones) showed more favorable enthalpic contributions and slightly higher affinity in comparison to compounds having the C2 linker (compound **3**) when the same fragment was attached. This indicated that the more flexible linker allows for a better orientation of the fragment leading to a more favorable enthalpy of binding, but also increases the entropic cost of binding, leading only to a moderate difference in the overall binding energy.

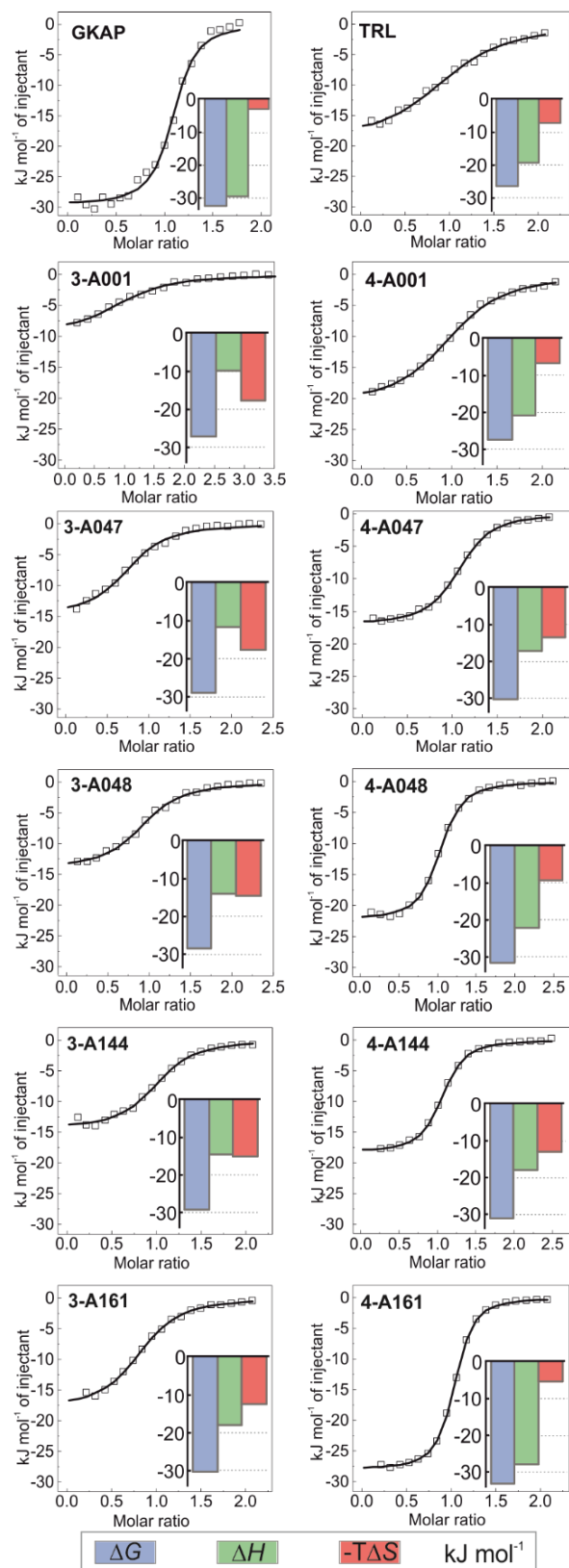


**Figure 4.** Hit validation by ITC. Fitted thermograms and thermodynamic signatures for the tested peptides and hydrazones. ITC data were acquired in 25 mM Tris, pH 7.5 buffer containing 150 mM NaCl at 25 °C by injecting 0.75-1mM peptide or hydrazone solution into 75-150  $\mu$ M protein in the cell. For individual raw ITC data and fitted thermograms see Figure S14.

Based on its affinity and the thermodynamic signature, compound **4-161** was identified as the best mimic of the wild-type sequence. It should be noted that the fragment in this hybrid is racemic, therefore the binding affinity must be the average of the two stereoisomers. It is worth noting that although compound **4-161** possessed the highest binding affinity, compound **4-A048** or **4-A144** have slightly higher ligand efficiencies and may therefore represent equally reasonable starting points for further optimization.

**Table 1.** Thermodynamic parameters for the tested compounds binding to SHANK1 PDZ derived from the ITC experiments.

	<i>n</i>	<i>K<sub>D</sub></i> ( $\mu$ M)	$\Delta H$ (kJ/mol)	$\Delta S$ (J/molK)
<b>GKAP</b>	1.07 $\pm$ 0.01	2.0 $\pm$ 0.3	-29.6 $\pm$ 0.4	9.7
<b>TRL</b>	1.04 $\pm$ 0.02	23 $\pm$ 2	-19.3 $\pm$ 0.5	24.1
<b>3-A001</b>	1.04 $\pm$ 0.04	16 $\pm$ 3	-9.7 $\pm$ 0.6	59.0
<b>4-A001</b>	1.00 $\pm$ 0.03	14.8 $\pm$ 0.8	-20.9 $\pm$ 0.2	22.2
<b>3-A047</b>	0.94 $\pm$ 0.01	8 $\pm$ 1	-11.5 $\pm$ 0.4	59.1
<b>4-A047</b>	1.06 $\pm$ 0.01	4.6 $\pm$ 0.2	-17.1 $\pm$ 0.1	44.8
<b>3-A048</b>	1.03 $\pm$ 0.01	10 $\pm$ 1	-14.1 $\pm$ 0.3	48.4
<b>4-A048</b>	0.99 $\pm$ 0.01	3.1 $\pm$ 0.2	-22.3 $\pm$ 0.2	30.7
<b>3-A144</b>	1.00 $\pm$ 0.02	7.1 $\pm$ 0.9	-14.4 $\pm$ 0.2	50.1
<b>4-A144</b>	1.03 $\pm$ 0.01	3.1 $\pm$ 0.2	-18.3 $\pm$ 0.1	44.1
<b>3-A161</b>	0.84 $\pm$ 0.01	4.8 $\pm$ 0.4	-18.0 $\pm$ 0.3	41.3
<b>4-A161</b>	1.00 $\pm$ 0.00	1.54 $\pm$ 0.05	-28.0 $\pm$ 0.1	17.3

To obtain more insight on the molecular nature of the interaction between the peptide-fragment hybrids and SHANK1 PDZ, co-crystal structures were solved for compounds **3-A047**, **4-A047**, **3-A048**, and **4-A048** with SHANK1 PDZ at resolutions of 1.5-2.2 Å (Table S2). In all structures, hybrids bound to the anticipated binding site with a similar conformation to the wild type sequence within the core amino acid sequence (Figures S15-18), indicating that the peptide component of the hybrid indeed fulfils the role of an anchor directing fragments towards the protein surface. In all hybrids, the hydrazone bond existed in an *E* configuration with the aromatic ring of the fragment co-planar with the hydrazone. We observed different orientations of the fragments relative to the peptide component presumably allowed by the conformational flexibility of the linker region. This linker flexibility also resulted in high B-factors with some missing density around the fragment in

most of the structures. Although there is therefore slight uncertainty about the exact location of the fragments, we hypothesize that the key carboxylic acid moiety “dances” across a positively charged patch formed by R679, R736 and R743 on the protein surface (Figure 5), making transient charge-reinforced hydrogen-bonding and cation- $\pi$  interactions. In the crystal structures where strong electron density allowed determination of the location of the fragment, we observed that this motif interacted with a loop of a symmetry related protein in the crystals (Figure S17 and S18). To probe this behavior further, we determined the rotational correlation time ( $\tau_c$ ) of the SHANK1 PDZ protein in the absence/presence of ligand using NMR  $T_1$  and  $T_2$  relaxation experiments (Figure S19). These analyses indicated similar  $\tau_c$  values for apo-SHANK1 and SHANK1 in the presence of these compounds, meaning that the interaction in the X-ray structure most likely arises from a crystal packing specific interaction.

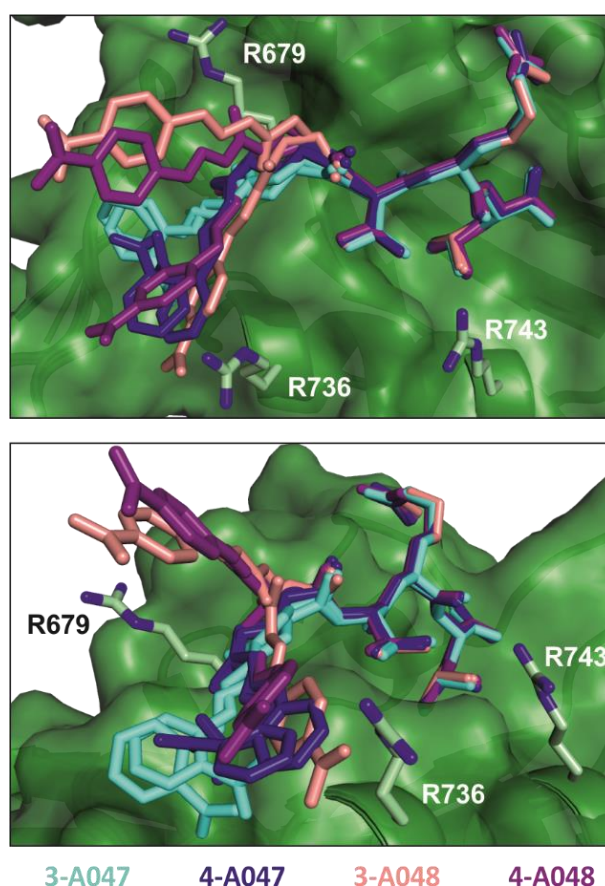


**Figure 5.** Superimposed crystal structure of **3-A047** (cyan, PDB: 6YWZ), **4-A047** (blue, PDB: 6YX1), **3-A048** (peach, PDB: 6YX0) and **4-A048** (purple, PDB: 6YX2) in complex with SHANK1 PDZ (green) showing two different orientations of the complexes. The core TRL sequence binds in a similar manner to the native wild-type ligand in both crystallographic protomers whilst the orientation of the acylhydrazone fragment component varies for each ligand and appears to “dance” around a series of basic residues (R679, R736, R743) at the periphery of the  $\beta$ -strand binding cleft on the PDZ domain.

To provide support for the hypothesis that the hybrids target the cationic patch on the surface of SHANK1, we performed molecular dynamics simulations on the SHANK1-compound **3-A048** complex using the crystal structure as a starting point. Over the course of three repeats of 200 ns, the aromatic carboxylate of the fragment indeed moves across the surface of the SHANK1 protein, making transient contacts with R679, R736 and R743, as well as intramolecular interaction onto the arginine in the peptide ligand to a lesser extent (see: supporting information, Movie S1). The distance between the carboxylate and these residues plotted against time over the course of the simulations (Figure S20) further indicates that the aromatic carboxylate is able to make transient non-covalent contacts in turn with each of the positively charged side-chains of the three arginine residues.

To further assess the selectivity of the peptide-fragment hybrids, we compared the ability to bind to SHANK1 against the ability to bind to the PDZ domain of PSD-95, a therapeutically important target in neuronal diseases and cancer.<sup>54</sup> We monitored the binding using chemical shift perturbations in the <sup>1</sup>H-<sup>15</sup>N HSQC spectra of the PDZ domain of PSD-95 (Figure S21-22 and Table S3-4). These analyses indicated weak binding with EC<sub>50</sub>=2.4 ± 0.3 mM for **4-A047** (Figure S23). The observed weak potency for the peptide-acylhydrazone fragment hybrids towards PSD-95 likely derives from its preference for Val or Ile at the C-terminus of its ligands.<sup>72</sup> However, PSD-95 also lacks the patch of cationic residues proximal to the C-terminal carboxylate binding site. Such a result provides confidence that the dynamic ligation screening approach used here can encode and retain selectivity.

## CONCLUSIONS

The identification of inhibitors of  $\beta$ -sheet mediated PPI interfaces, which are generally shallow and elongated, is extremely challenging. Here, we used dynamic ligation screening to identify peptide-fragment hybrids linked through an acylhydrazone bond, that are able to functionally mimic a  $\beta$ -strand and inhibit its PPI using GKAP/ SHANK1 PDZ as a model interaction. The identified ligands were shown to bind with comparable potency to the GKAP PBM (Ac-EAQTRL-COOH) ligand from which they were derived and were selective when tested against an alternative PDZ domain. Crystallographic studies supported by molecular dynamics analyses indicated that the fragment portion of the hybrids was able to reinforce SHANK1 recognition by engaging in transient charge-reinforced and cation- $\pi$  interactions on the protein surface, providing new insight on the molecular recognition of SHANK1 towards its peptide/protein ligands that can be used to inform chemical probes development – a focus of our future studies.

More generally, our approach is advantageous in that it allows *i)* use of commercially available aldehyde fragments to build a small, diverse library then extend it to near neighbors based on initial hits; *ii)* ligation to be performed under conditions where the reaction is reversible, and is compatible with the screening assay, *iii)* validate hits easily without the need for a further synthetic step, thus providing useful insights on structure-activity relationships and *iv)* explore unoccupied binding sites on a protein surface in an unbiased manner to generate ligands with target affinity and selectivity. Significantly, whilst reversible protein-directed fragment discovery in the form of disulfide-tethering has been used to develop modulators of PPIs,<sup>73-75</sup> the use of ligand-directed fragment discovery to develop modulators of PPIs has not been widely developed. Thus, these proof-of concept results exemplified here point to future application of dynamic-ligation screening to identify and optimize PPI modulators more broadly.

### **Supporting Information.**

Supporting figures and Schemes, Peptide characterization data, materials and methods.

### **Corresponding Author**

\* a.j.wilson@leeds.ac.uk

### **Present Addresses**

† Z. Hegedus

Department of Medical Chemistry, Faculty of Medicine, University of Szeged, Dóm tér 8., Szeged, 6720, Hungary

### **Author Contributions**

Z.H, T. A. E and A.J.W. conceived and designed the research program, Z.H. designed studies and performed the research with support from F. H. and L-Y. L. (NMR), S.C (synthesis) and C.H.T. (crystallography). D.S and R.B. S. performed molecular dynamics analyses. The manuscript was written by Z.H. and A.J.W. with contributions from all authors. Z. H. prepared all figures.

### **ACKNOWLEDGMENT**

This project has received funding from the European Union's Horizon 2020 research and innovation programme under the Marie Skłodowska-Curie grant agreement no. MSCA-IF-2016-749012. This work was supported by EPSRC (EP/N035267/1) and the BBSRC/EPSRC-funded Synthetic Biology Research Centre, BrisSynBio (BB/L01386X/1). AJW holds a Royal Society Leverhulme Trust Senior Fellowship (SRF/R1/191087). We acknowledge Diamond Light Source for time on Beamline I03, I04 and I24 under Proposal mx19248 and the authors would like to thank the staff of these beamlines for assistance with data collection.

## REFERENCES

- (1) Nussinov, R.; Tsai, C. J. Allostery in Disease and in Drug Discovery. *Cell* **2013**, *153* (2), 293–305.
- (2) Keskin, O.; Gursoy, A.; Ma, B.; Nussinov, R. Principles of Protein-Protein Interactions: What Are the Preferred Ways for Proteins to Interact? *Chem. Rev.* **2008**, *108* (4), 1225–1244.
- (3) Arrowsmith, C. H.; Audia, J. E.; Austin, C.; Baell, J.; Bennett, J.; Blagg, J.; Bountra, C.; Brennan, P. E.; Brown, P. J.; Bunnage, M. E.; Buser-Doepner, C.; Campbell, R. M.; Carter, A. J.; Cohen, P.; Copeland, R. A.; Cravatt, B.; Dahlin, J. L.; Dhanak, D.; Edwards, A. M.; Frye, S. V.; Gray, N.; Grimshaw, C. E.; Hepworth, D.; Howe, T.; Huber, K. V. M.; Jin, J.; Knapp, S.; Kotz, J. D.; Kruger, R. G.; Lowe, D.; Mader, M. M.; Marsden, B.; Mueller-Fahrnow, A.; Müller, S.; O'Hagan, R. C.; Overington, J. P.; Owen, D. R.; Rosenberg, S. H.; Roth, B.; Ross, R.; Schapira, M.; Schreiber, S. L.; Shoichet, B.; Sundström, M.; Superti-Furga, G.; Taunton, J.; Toledo-Sherman, L.; Walpole, C.; Walters, M. A.; Willson, T. M.; Workman, P.; Young, R. N.; Zuercher, W. J. The Promise and Peril of Chemical Probes. *Nat. Chem. Biol.* **2015**, *11* (8), 536–541.
- (4) Andrei, S. A.; Sijbesma, E.; Hann, M.; Davis, J.; O'Mahony, G.; Perry, M. W. D.; Karawajczyk, A.; Eickhoff, J.; Brunsveld, L.; Doveston, R. G.; Milroy, L. G.; Ottmann, C. Stabilization of Protein-Protein Interactions in Drug Discovery. *Expert Opin. Drug Discov.* **2017**, *12* (9), 925–940.
- (5) Arkin, M. R.; Tang, Y.; Wells, J. A. Small-Molecule Inhibitors of Protein-Protein Interactions: Progressing toward the Reality. *Chem. Biol.* **2014**, *21* (9), 1102–1114.
- (6) Scott, D. E.; Bayly, A. R.; Abell, C.; Skidmore, J. Small Molecules, Big Targets: Drug Discovery Faces the Protein-Protein Interaction Challenge. *Nat. Rev. Drug Discovery* **2016**, *15* (8), 533–550.
- (7) Roberts, A. W.; Davids, M. S.; Pagel, J. M.; Kahl, B. S.; Puvvada, S. D.; Gerecitano, J. F.; Kipps, T. J.; Anderson, M. A.; Brown, J. R.; Gressick, L.; Wong, S.; Dunbar, M.; Zhu, M.; Desai, M. B.; Cerri, E.; Enschede, S. H.; Humerickhouse, R. A.; Wierda, W. G.; Seymour, J. F. Targeting BCL2 with Venetoclax in Relapsed Chronic Lymphocytic Leukemia. *N. Engl. J. Med.* **2016**, *374* (4), 311–322.
- (8) Tompa, P.; Davey, N. E.; Gibson, T. J.; Babu, M. M. A Million Peptide Motifs for the Molecular Biologist. *Mol. Cell* **2014**, *55* (2), 161–169.
- (9) Ivarsson, Y.; Jemth, P. Affinity and Specificity of Motif-Based Protein-Protein Interactions. *Curr. Opin. Struct. Biol.* **2019**, *54*, 26–33.
- (10) Ran, X.; Gestwicki, J. E. Inhibitors of Protein-Protein Interactions (PPIs): An Analysis of Scaffold Choices and Buried Surface Area. *Curr. Opin. Chem. Biol.* **2018**, *44*, 75–86.
- (11) Merritt, H. I.; Sawyer, N.; Arora, P. S. Bent into Shape: Folded Peptides to Mimic Protein Structure and Modulate Protein Function. *Pept. Sci.* **2020**, *112*, e24145.
- (12) Outlaw, V. K.; Lemke, J. T.; Zhu, Y.; Gellman, S. H.; Porotto, M.; Moscona, A. Structure-Guided Improvement of a Dual HPIV3/RSV Fusion Inhibitor. *J. Am. Chem. Soc.* **2020**, *142* (5), 2140–2144.
- (13) Watkins, A. M.; Arora, P. S. Anatomy of  $\beta$ -Strands at Protein-Protein Interfaces. *ACS Chem. Biol.* **2014**, *9* (8), 1747–1754.
- (14) German, E. A.; Ross, J. E.; Knipe, P. C.; Don, M. F.; Thompson, S.; Hamilton, A. D. B-Strand Mimetic Foldamers Rigidified Through Dipolar Repulsion. *Angew. Chem., Int. Ed.* **2015**, *54* (9), 2649–2652.
- (15) Lingard, H.; Han, J. T.; Thompson, A. L.; Leung, I. K. H.; Scott, R. T. W.; Thompson, S.; Hamilton, A. D. Diphenylacetylene-Linked Peptide Strands Induce Bidirectional  $\beta$ -Sheet Formation. *Angew. Chem., Int. Ed.* **2014**, *53* (14), 3650–3653.
- (16) Matsumoto, M.; Lee, S. J.; Waters, M. L.; Gagné, M. R. A Catalyst Selection Protocol That Identifies Biomimetic Motifs from  $\beta$ -Hairpin Libraries. *J. Am. Chem. Soc.* **2014**, *136* (45), 15817–15820.
- (17) Fülöp, L.; Mándity, I. M.; Juhász, G.; Szegedi, V.; Hetényi, A.; Wéber, E.; Bozsó, Z.; Simon, D.; Benko, M.; Király, Z.; Martinek, T. A. A Foldamer-Dendrimer Conjugate Neutralizes Synaptotoxic  $\beta$ -Amyloid Oligomers. *PLoS One* **2012**, *7* (7), e39485.
- (18) Thomas, N. C.; Bartlett, G. J.; Woolfson, D. N.; Gellman, S. H. Toward a Soluble Model System for the Amyloid State. *J. Am. Chem. Soc.* **2017**, *139* (46), 16434–16437.
- (19) Kreutzer, A. G.; Nowick, J. S. Elucidating the Structures of Amyloid Oligomers with Macrocylic  $\beta$ -Hairpin

- Peptides: Insights into Alzheimer's Disease and Other Amyloid Diseases. *Acc. Chem. Res.* **2018**, *51* (3), 706–718.
- (20) Kang, C. W.; Sarnowski, M. P.; Ranatunga, S.; Wojtas, L.; Metcalf, R. S.; Guida, W. C.; Del Valle, J. R.  $\beta$ -Strand Mimics Based on Tetrahydropyridazinedione (Tpd) Peptide Stitching. *Chem. Commun.* **2015**, *51* (90), 16259–16262.
- (21) Sarnowski, M. P.; Kang, C. W.; Elbatrawi, Y. M.; Wojtas, L.; Del Valle, J. R. Peptide N-Amination Supports  $\beta$ -Sheet Conformations. *Angew. Chemie Int. Ed.* **2017**, *56* (8), 2083–2086.
- (22) Zheng, J.; Baghkhani, A. M.; Nowick, J. S. A Hydrophobic Surface Is Essential to Inhibit the Aggregation of a Tau-Protein-Derived Hexapeptide. *J. Am. Chem. Soc.* **2013**, *135* (18), 6846–6852.
- (23) Angelo, N. G.; Arora, P. S. Nonpeptidic Foldamers from Amino Acids: Synthesis and Characterization of 1,3-Substituted Triazole Oligomers. *J. Am. Chem. Soc.* **2005**, *127* (49), 17134–17135.
- (24) Rzepecki, P.; Gallmeier, H.; Geib, N.; Cernovska, K.; König, B.; Schrader, T. New Heterocyclic  $\beta$ -Sheet Ligands with Peptidic Recognition Elements. *J. Org. Chem.* **2004**, *69* (16), 5168–5178.
- (25) Jamieson, A. G.; Russell, D.; Hamilton, A. D. A 1,3-Phenyl-Linked Hydantoin Oligomer Scaffold as a  $\beta$ -Strand Mimetic. *Chem. Commun.* **2012**, *48* (31), 3709–3711.
- (26) Hammond, M. C.; Harris, B. Z.; Lim, W. A.; Bartlett, P. A.  $\beta$  Strand Peptidomimetics as Potent PDZ Domain Ligands. *Chem. Biol.* **2006**, *13* (12), 1247–1251.
- (27) Cheng, P. N.; Liu, C.; Zhao, M.; Eisenberg, D.; Nowick, J. S. Amyloid  $\beta$ -Sheet Mimics That Antagonize Protein Aggregation and Reduce Amyloid Toxicity. *Nat. Chem.* **2012**, *4* (11), 927–933.
- (28) Zutshi, R.; Franciskovich, J.; Shultz, M.; Schweitzer, B.; Bishop, P.; Wilson, M.; Chmielewski, J. Targeting the Dimerization Interface of HIV-1 Protease: Inhibition with Cross-Linked Interfacial Peptides. *J. Am. Chem. Soc.* **1997**, *119* (21), 4841–4845.
- (29) Pelay-Gimeno, M.; Glas, A.; Koch, O.; Grossmann, T. N. Structure-Based Design of Inhibitors of Protein-Protein Interactions: Mimicking Peptide Binding Epitopes. *Angew. Chem., Int. Ed.* **2015**, *54* (31), 8896–8927.
- (30) Kontopidis, G.; Andrews, M. J.; McInnes, C.; Plater, A.; Innes, L.; Renachowski, S.; Cowan, A.; Fischer, P. M. Truncation and Optimisation of Peptide Inhibitors of Cyclin-Dependent Kinase 2-Cyclin A through Structure-Guided Design. *ChemMedChem* **2009**, *4* (7), 1120–1128.
- (31) Liu, S.; Premnath, P. N.; Bolger, J. K.; Perkins, T. L.; Kirkland, L. O.; Kontopidis, G.; McInnes, C. Optimization of Non-ATP Competitive CDK/Cyclin Groove Inhibitors through REPLACE-Mediated Fragment Assembly. *J. Med. Chem.* **2013**, *56* (4), 1573–1582.
- (32) Premnath, P. N.; Craig, S. N.; Liu, S.; McInnes, C. Benzamide Capped Peptidomimetics as Non-ATP Competitive Inhibitors of CDK2 Using the REPLACE Strategy. *Bioorg. Med. Chem. Lett.* **2016**, *26* (15), 3754–3760.
- (33) Andrews, M. J. I.; Kontopidis, G.; McInnes, C.; Plater, A.; Innes, L.; Cowan, A.; Jewsbury, P.; Fischer, P. M. REPLACE: A Strategy for Iterative Design of Cyclin-Binding Groove Inhibitors. *ChemBioChem* **2006**, *7* (12), 1909–1915.
- (34) Premnath, P. N.; Craig, S. N.; Liu, S.; Anderson, E. L.; Grigoroudis, A. I.; Kontopidis, G.; Perkins, T. L.; Wyatt, M. D.; Pittman, D. L.; McInnes, C. Iterative Conversion of Cyclin Binding Groove Peptides into Druglike CDK Inhibitors with Antitumor Activity. *J. Med. Chem.* **2015**, *58* (1), 433–442.
- (35) Beekman, A. M.; O'Connell, M. A.; Howell, L. A. Peptide-Directed Binding for the Discovery of Modulators of  $\alpha$ -Helix-Mediated Protein-Protein Interactions: Proof-of-Concept Studies with the Apoptosis Regulator Mcl-1. *Angew. Chem., Int. Ed.* **2017**, *56* (35), 10446–10450.
- (36) Beekman, A. M.; Cominetti, M. M. D.; Walpole, S. J.; Prabhu, S.; O'Connell, M. A.; Angulo, J.; Searcey, M. Identification of Selective Protein-Protein Interaction Inhibitors Using Efficient: In Silico Peptide-Directed Ligand Design. *Chem. Sci.* **2019**, *10* (16), 4502–4508.
- (37) Unver, M. Y.; Gierse, R. M.; Ritchie, H.; Hirsch, A. K. H. Druggability Assessment of Targets Used in Kinetic Target-Guided Synthesis. *J. Med. Chem.* **2018**, *61* (21), 9395–9409.
- (38) Jaegle, M.; Wong, E. L.; Tauber, C.; Nawrotzky, E.; Arkona, C.; Rademann, J. Protein-Templated Fragment Ligations—From Molecular Recognition to Drug Discovery. *Angew. Chem., Int. Ed.* **2017**, *56* (26), 7358–7378.
- (39) Chung, M. K.; White, P. S.; Lee, S. J.; Waters, M. L.; Gagné, M. R. Self-Assembled Multi-Component Catenanes: Structural Insights into an Adaptable Class of Molecular Receptors and [2]-Catenanes. *J. Am. Chem. Soc.* **2012**, *134* (28), 11415–11429.
- (40) Chung, M. K.; White, P. S.; Lee, S. J.; Gagné, M. R.; Waters, M. L. Investigation of a Catenane with a Responsive Noncovalent Network: Mimicking Long-Range Responses in Proteins. *J. Am. Chem. Soc.* **2016**, *138* (40), 13344–

13352.

- (41) Chung, M. K.; Lee, S. J.; Waters, M. L.; Gagné, M. R. Self-Assembled Multi-Component Catenanes: The Effect of Multivalency and Cooperativity on Structure and Stability. *J. Am. Chem. Soc.* **2012**, *134* (28), 11430–11443.
- (42) Rooklin, D.; Modell, A. E.; Li, H.; Berdan, V.; Arora, P. S.; Zhang, Y. Targeting Unoccupied Surfaces on Protein-Protein Interfaces. *J. Am. Chem. Soc.* **2017**, *139* (44), 15560–15563.
- (43) Schmidt, M. F.; El-Dahshan, A.; Keller, S.; Rademann, J. Selective Identification of Cooperatively Binding Fragments in a High-Throughput Ligation Assay Enables Development of a Picomolar Caspase-3 Inhibitor. *Angew. Chem., Int. Ed.* **2009**, *48* (34), 6346–6349.
- (44) Schmidt, M. F.; Isidro-Llobet, A.; Lisurek, M.; El-Dahshan, A.; Tan, J.; Hilgenfeld, R.; Rademann, J. Sensitized Detection of Inhibitory Fragments and Iterative Development of Non-Peptidic Protease Inhibitors by Dynamic Ligation Screening. *Angew. Chem., Int. Ed.* **2008**, *47* (17), 3275–3278.
- (45) Mondal, M.; Radeva, N.; Fanlo-Virgós, H.; Otto, S.; Klebe, G.; Hirsch, A. K. H. Fragment Linking and Optimization of Inhibitors of the Aspartic Protease Endothiapepsin: Fragment-Based Drug Design Facilitated by Dynamic Combinatorial Chemistry. *Angew. Chem., Int. Ed.* **2016**, *55* (32), 9422–9426.
- (46) Im, Y. J.; Lee, J. H.; Park, S. H.; Park, S. J.; Rho, S. H.; Kang, G. B.; Kim, E.; Eom, S. H. Crystal Structure of the Shank PDZ-Ligand Complex Reveals a Class I PDZ Interaction and a Novel PDZ-PDZ Dimerization. *J. Biol. Chem.* **2003**, *278* (48), 48099–48104.
- (47) Monteiro, P.; Feng, G. SHANK Proteins: Roles at the Synapse and in Autism Spectrum Disorder. *Nat. Rev. Neurosci.* **2017**, *18* (3), 147–157.
- (48) Ernst, A.; Appleton, B. A.; Ivarsson, Y.; Zhang, Y.; Gfeller, D.; Wiesmann, C.; Sidhu, S. S. A Structural Portrait of the PDZ Domain Family. *J. Mol. Biol.* **2014**, *426* (21), 3509–3519.
- (49) Ye, F.; Zhang, M. Structures and Target Recognition Modes of PDZ Domains: Recurring Themes and Emerging Pictures. *Biochem. J.* **2013**, *455* (1), 1–14.
- (50) Zhang, M.; Wang, W. Organization of Signaling Complexes by PDZ-Domain Scaffold Proteins. *Acc. Chem. Res.* **2003**, *36* (7), 530–538.
- (51) Hajduk, P. J.; Huth, J. R.; Fesik, S. W. Druggability Indices for Protein Targets Derived from NMR-Based Screening Data. *J. Med. Chem.* **2005**, *48* (7), 2518–2525.
- (52) Ivarsson, Y.; Arnold, R.; McLaughlin, M.; Nim, S.; Joshi, R.; Ray, D.; Liu, B.; Teyra, J.; Pawson, T.; Moffat, J.; Li, S. S. C.; Sidhu, S. S.; Kim, P. M. Large-Scale Interaction Profiling of PDZ Domains through Proteomic Peptide-Phage Display Using Human and Viral Phage Peptidomes. *Proc. Natl. Acad. Sci. U. S. A.* **2014**, *111* (7), 2542–2547.
- (53) Rimbault, C.; Maruthi, K.; Breillat, C.; Genuer, C.; Crespillo, S.; Puente-Muñoz, V.; Chamma, I.; Gauthereau, I.; Antoine, S.; Thibaut, C.; Tai, F. W. J.; Dartigues, B.; Grillo-Bosch, D.; Claverol, S.; Poujol, C.; Choquet, D.; Mackereth, C. D.; Sainlos, M. Engineering Selective Competitors for the Discrimination of Highly Conserved Protein-Protein Interaction Modules. *Nat. Commun.* **2019**, *10* (1), 1–20.
- (54) Bach, A.; Clausen, B. H.; Møller, M.; Vestergaard, B.; Chi, C. N.; Round, A.; Sørensen, P. L.; Nissen, K. B.; Kastrop, J. S.; Gajhede, M.; Jemth, P.; Kristensen, A. S.; Lundström, P.; Lambertsen, K. L.; Strømgaard, K. A High-Affinity, Dimeric Inhibitor of PSD-95 Bivalently Interacts with PDZ1-2 and Protects against Ischemic Brain Damage. *Proc. Natl. Acad. Sci. U. S. A.* **2012**, *109* (9), 3317–3322.
- (55) Sainlos, M.; Tigaret, C.; Poujol, C.; Olivier, N. B.; Bard, L.; Breillat, C.; Thiolon, K.; Choquet, D.; Imperiali, B. Biomimetic Divalent Ligands for the Acute Disruption of Synaptic AMPAR Stabilization. *Nat. Chem. Biol.* **2011**, *7* (2), 81–91.
- (56) Udagamasooriya, D. G.; Sharma, S. C.; Spaller, M. R. A Chemical Library Approach to Organic-Modified Peptide Ligands for PDZ Domain Proteins: A Synthetic, Thermodynamic and Structural Investigation. *ChemBioChem* **2008**, *9* (10), 1587–1589.
- (57) Piserchio, A.; Salinas, G. D.; Li, T.; Marshall, J.; Spaller, M. R.; Mierke, D. F. Targeting Specific PDZ Domains of PSD-95: Structural Basis for Enhanced Affinity and Enzymatic Stability of a Cyclic Peptide. *Chem. Biol.* **2004**, *11* (4), 469–473.
- (58) Bach, A.; Eildal, J. N. N.; Stühr-Hansen, N.; Deeskamp, R.; Gottschalk, M.; Pedersen, S. W.; Kristensen, A. S.; Strømgaard, K. Cell-Permeable and Plasma-Stable Peptidomimetic Inhibitors of the Postsynaptic Density-95/N-Methyl-D-Aspartate Receptor Interaction. *J. Med. Chem.* **2011**, *54* (5), 1333–1346.
- (59) Chi, C. N.; Bach, A.; Strømgaard, K.; Gianni, S.; Jemth, P. Ligand Binding by PDZ Domains. *BioFactors* **2012**, *38*

- (5), 338–348.
- (60) Thorsen, T. S.; Madsen, K. L.; Rebola, N.; Rathje, M.; Anggono, V.; Bach, A.; Moreira, I. S.; Stuhr-Hansen, N.; Dyhring, T.; Peters, D.; Beuming, T.; Hugarir, R.; Weinstein, H.; Mülle, C.; Strømgaard, K.; Rønn, L. C. B.; Gether, U. Identification of a Small-Molecule Inhibitor of the PICK1 PDZ Domain That Inhibits Hippocampal LTP and LTD. *Proc. Natl. Acad. Sci. U. S. A.* **2010**, *107* (1), 413–418.
- (61) Saupe, J.; Roske, Y.; Schillinger, C.; Kamdem, N.; Radetzki, S.; Diehl, A.; Oschkinat, H.; Krause, G.; Heinemann, U.; Rademann, J. Discovery, Structure-Activity Relationship Studies, and Crystal Structure of Nonpeptide Inhibitors Bound to the Shank3 PDZ Domain. *ChemMedChem* **2011**, *6* (8), 1411–1422.
- (62) Shan, J.; Zhang, X.; Bao, J.; Cassell, R.; Zheng, J. J. Synthesis of Potent Dishevelled PDZ Domain Inhibitors Guided by Virtual Screening and NMR Studies. *Chem. Biol. Drug Des.* **2012**, *79* (4), 376–383.
- (63) Bhat, V. T.; Caniard, A. M.; Luksch, T.; Brenk, R.; Campopiano, D. J.; Greaney, M. F. Nucleophilic Catalysis of Acylhydrazone Equilibration for Protein-Directed Dynamic Covalent Chemistry. *Nat. Chem.* **2010**, *2* (6), 490–497.
- (64) Larsen, D.; Kietrys, A. M.; Clark, S. A.; Park, H. S.; Ekebergh, A.; Kool, E. T. Exceptionally Rapid Oxime and Hydrazone Formation Promoted by Catalytic Amine Buffers with Low Toxicity. *Chem. Sci.* **2018**, *9* (23), 5252–5259.
- (65) Kalia, J.; Raines, R. T. Hydrolytic Stability of Hydrazones and Oximes. *Angew. Chemie Int. Ed.* **2008**, *47* (39), 7523–7526.
- (66) Bunyapaiboonsri, T.; Ramström, O.; Lohmann, S.; Lehn, J. M.; Peng, L.; Goeldner, M. Dynamic Deconvolution of a Pre-Equilibrated Dynamic Combinatorial Library of Acetylcholinesterase Inhibitors. *ChemBioChem* **2001**, *2* (6), 438–444.
- (67) Ye, F.; Zhang, M. Structures and Target Recognition Modes of PDZ Domains: Recurring Themes and Emerging Pictures. *Biochem. J.* **2013**, *455* (1), 1–14.
- (68) Ibarra, A. A.; Bartlett, G. J.; Hegedüs, Z.; Dutt, S.; Hobor, F.; Horner, K. A.; Hetherington, K.; Spence, K.; Nelson, A.; Edwards, T. A.; Woolfson, D. N.; Sessions, R. B.; Wilson, A. J. Predicting and Experimentally Validating Hot-Spot Residues at Protein-Protein Interfaces. *ACS Chem. Biol.* **2019**, *14* (10), 2252–2263.
- (69) Lee, J. H.; Park, H. J.; Park, S. J.; Kim, H. J.; Eom, S. H. The Structural Flexibility of the Shank1 PDZ Domain Is Important for Its Binding to Different Ligands. *Biochem. Biophys. Res. Commun.* **2011**, *407* (1), 207–212.
- (70) Davey, N. E.; Seo, M. H.; Yadav, V. K.; Jeon, J.; Nim, S.; Krystkowiak, I.; Blikstad, C.; Dong, D.; Markova, N.; Kim, P. M.; Ivarsson, Y. Discovery of Short Linear Motif-Mediated Interactions through Phage Display of Intrinsically Disordered Regions of the Human Proteome. *FEBS J.* **2017**, *284* (3), 485–498.
- (71) Jhoti, H.; Williams, G.; Rees, D. C.; Murray, C. W. The “rule of Three” for Fragment-Based Drug Discovery: Where Are We Now? *Nat. Rev. Drug Discovery* **2013**, *12* (8), 644.
- (72) Cohen, N. A.; Brenman, J. E.; Snyder, S. H.; Brecht, D. S. Binding of the Inward Rectifier K<sup>+</sup> Channel Kir 2.3 to PSD-95 Is Regulated by Protein Kinase A Phosphorylation. *Neuron* **1996**, *17* (4), 759–767.
- (73) Ostrem, J. M.; Peters, U.; Sos, M. L.; Wells, J. A.; Shokat, K. M. K-Ras(G12C) Inhibitors Allosterically Control GTP Affinity and Effector Interactions. *Nature* **2013**, *503* (7477), 548–551.
- (74) Wang, N.; Majmudar, C. Y.; Pomerantz, W. C.; Gagnon, J. K.; Sadowsky, J. D.; Meagher, J. L.; Johnson, T. K.; Stuckey, J. A.; Brooks, C. L.; Wells, J. A.; Mapp, A. K. Ordering a Dynamic Protein Via a Small-Molecule Stabilizer. *J. Am. Chem. Soc.* **2013**, *135* (9), 3363–3366.
- (75) Sijbesma, E.; Hallenbeck, K. K.; Leysen, S.; De Vink, P. J.; Skóra, L.; Jahnke, W.; Brunsveld, L.; Arkin, M. R.; Ottmann, C. Site-Directed Fragment-Based Screening for the Discovery of Protein-Protein Interaction Stabilizers. *J. Am. Chem. Soc.* **2019**, *141* (8), 3524–3531.

Dynamic ligation screening of peptide-acylhydrazones was used to identify peptide-fragment hybrids that act as functional  $\beta$ -strand mimics to selectively inhibit the interaction between a peptide binding motif from GKAP and the PDZ domain of SHANK1. Inhibition was achieved by retaining key recognition features of the core peptide sequence and augmenting these with dynamic interactions of the identified carboxylate bearing fragment with a cationic patch on SHANK1 proximal to the core recognition interface as demonstrated by biophysical and structural methods.

